NeuroImage 79 (2013) 1–9

Contents lists available at SciVerse ScienceDirect

NeuroImage

journal homepage: www.elsevier.com/locate/ynimg

Selectivity for large nonmanipulable objects in scene-selective visual cortex does not require visual experience

Chenxi He [a], Marius V. Peelen [b,c], Zaizhu Han [a], Nan Lin [a], Alfonso Caramazza [b,c], Yanchao Bi [a,*]

[a] State Key Laboratory of Cognitive Neuroscience and Learning, Beijing Normal University, China
[b] Center for Mind/Brain Sciences, University of Trento, Italy
[c] Department of Psychology, Harvard University, USA

ARTICLE INFO

Article history:
Accepted 15 April 2013
Available online 25 April 2013

Keywords:
Congenitally blind
Object representation
Ventral temporal cortex
Scene-selective
Parahippocampal place area

ABSTRACT

The principles that determine the organization of object representations in ventral temporal cortex (VTC) remain elusive. Here, we focus on the parahippocampal place area (PPA), a region in medial VTC that has been shown to respond selectively to pictures of scenes. Recent studies further observed that this region also shows a preference for large nonmanipulable objects relative to other objects, which might reflect the suitability of large objects for navigation. The mechanisms underlying this selectivity remain poorly understood. We examined the extent to which PPA selectivity requires visual experience. Fourteen congenitally blind and matched sighted participants were tested on an auditory size judgment experiment involving large nonmanipulable objects, small objects (tools), and animals. Sighted participants additionally participated in a picture-viewing experiment. Replicating previous work, we found that the PPA responded selectively to large nonmanipulable objects, relative to tools and animals, in the sighted group viewing pictures. Importantly, this selectivity was also observed in the auditory experiment in both sighted and congenitally blind groups. In both groups, selectivity for large nonmanipulable objects was additionally observed in the retrosplenial complex (RSC) and the transverse occipital sulcus (TOS), regions previously implicated in scene perception and navigation. Finally, in both groups the PPA showed resting-state functional connectivity with TOS and RSC. These results provide new evidence that large object selectivity in PPA, and the intrinsic connectivity between PPA and other navigation-relevant regions, do not require visual experience. More generally, they show that the organization of object representations in VTC can develop, at least partly, without visual experience.

Introduction

The functional organization of object representations in the human visual cortex, especially the ventral temporal cortex (VTC), has been the focus of much recent research. Functional neuroimaging studies have provided evidence that different object domains evoke distinct responses in VTC. For example, specific regions of VTC respond selectively to particular object categories, such as faces, bodies, words, or places (Bracci et al., 2010; Chao et al., 1999; Cohen and Dehaene, 2004; Downing et al., 2001, 2006; Epstein and Kanwisher, 1998; Kanwisher, 2010; Kanwisher et al., 1997; Peelen and Downing, 2005).

A particularly strong type of categorical selectivity is observed with scene stimuli. Compared to pictures of faces, common objects or scrambled pictures, pictures of scenes or places elicit stronger activation in a region in the parahippocampal gyrus (the parahippocampal place area, PPA), along with two additional regions in the retrosplenial complex (RSC) and the transverse occipital sulcus (TOS) (e.g., Epstein and Kanwisher, 1998; Goh et al., 2004). These findings motivated hypotheses about the function of PPA, including that it processes peripheral visual information, certain geometrical features about openness or closeness, or spatial properties (e.g., Kravitz et al., 2011; Levy et al., 2001; Park et al., 2011; Ross and Oliva, 2010). Interestingly, a series of recent studies showed that PPA activity is also modulated by the type of objects, preferring objects that are part of a scene (e.g., buildings, Maguire et al., 2001), large (Konkle and Oliva, 2012; Mullally and Maguire, 2011; Troiano et al., in press), with strong contextual associations (e.g., Bar and Aminoff, 2003), or those that more easily evoke a sense of space or place (Mullally and Maguire, 2011).

The degree to which visual object properties underlie the observed object categorical effects in PPA remains debated. One type of proposal is that the preference for scenes and some types of objects is driven by its sensitivity to certain visual aspects that are shared between scenes and these objects, e.g., peripheral visual information being more important (e.g., Konkle and Oliva, 2012). Alternatively, it might be because these regions are at least partly engaged in the more abstract interpretation of the stimulus, and the selectivity reflects how strongly the objects imply a scene/place and information useful for spatial navigation (e.g., Troiano et al., in press). In the

* Corresponding author at: State Key Laboratory of Cognitive Neuroscience and Learning, Beijing Normal University, Beijing 100875, PR China. Fax: +86 10 5880 2911.
E-mail address: ybi@bnu.edu.cn (Y. Bi).

1053-8119/$ – see front matter © 2013 Elsevier Inc. All rights reserved.
http://dx.doi.org/10.1016/j.neuroimage.2013.04.051

present study we tested congenitally blind participants to investigate whether knowledge of visual object properties is required for object category selectivity in the PPA.

While the potentially relevant object properties driving PPA, such as size, are predominantly obtained through the visual modality in normal circumstances, they can nonetheless be obtained through other modalities. Save et al. (1998) reported that early blind rats exhibited place cell firing activities highly similar to sighted rats. In humans, Wolbers et al. (2011) reported that both blind and sighted participants showed stronger PPA activation when they explored Legos as a scene layout compared to when they explored the stimuli as objects, suggesting that PPA's engagement in scene processing can develop without visual experience.

Other aspects of object categorical distributions in VTC have also been shown to be independent of visual experience. Pietrini et al. (2004) reported category-related fMRI response patterns for faces and manmade objects in VTC in congenitally blind participants during tactile object recognition. Reich et al. (2011) found that congenitally blind individuals show selective fMRI responses to Braille word stimuli in a region in left VTC that closely corresponds to the "visual word form area" in sighted individuals. Mahon et al. (2009) observed a preference for inanimate over animate objects in the medial portion of bilateral VTC in both sighted and three congenitally blind participants performing an auditory size judgment task.

In the present study, we investigated whether the selectivity for large nonmanipulable objects in PPA requires previous visual experience. We compared PPA responses to objects that are large and typically nonmanipulable/nonportable, relative to small manipulable objects (tools) and animals in sighted and congenitally blind participants. Both participant groups listened to the names of these objects, and sighted participants additionally viewed pictures. If the selectivity to large nonmanipulable objects in PPA was driven primarily by certain visual properties specifically associated with these objects, we expect that congenitally blind participants would show different (i.e., weaker, null, or disordered) patterns in comparison to the sighted participants. If, however, such selectivity in PPA originated from non-visual processes such as multi-modal spatial navigation, we expect that congenitally blind participants would develop PPA selectivity patterns similar to sighted participants. Furthermore, to better understand the role of visual experience in shaping PPA's functional profile, we explored the intrinsic functional connectivity pattern of PPA using resting-state fMRI in both participant groups, aiming to examine whether the spontaneous functional network associated with PPA is affected by visual experience.

Methods

Participants

Sixteen congenitally blind and seventeen sighted adults were scanned and paid for participation in the study. All blind participants reported that they lost their vision since birth, ten due to major retinal damage and six not knowing the exact pathology. Seven of them had faint light perception but could not recognize any pattern. Two blind individuals were excluded from the data analysis because the MRI scans discovered unknown old brain lesions. One sighted participant was discarded from the experimental data analysis due to excessive head motion during the experimental run. The remaining fourteen blind and sixteen sighted participants were matched on gender distribution (blind: seven females; sighted: seven females), handedness (all right handed), age (blind: mean = 45, SD = 10, range = 26–60; sighted: mean = 38, SD = 12, range = 18–60; $t(28) = 1.6$, $p = .11$) and years of education (blind: mean = 11, SD = 2, range = 9–12; sighted: mean = 11, SD = 2, range = 9–12; $t(28) < 1$). They were all native Mandarin Chinese speakers. None suffered from psychiatric or neurological disorders, had ever sustained head injury, or were on any psychoactive medications. All participants completed a written informed consent approved by the institutional review board of Beijing Normal University (BNU) Imaging Center for Brain Research.

Materials and procedure

Congenitally blind and sighted participants performed an auditorily-presented task. In the same session we also included a picture-viewing task in which the sighted participants viewed the same objects as the items used in the auditory experiment. In a separate session, carried out at a later time, a scene localizer task was administered to four of the sighted participants to functionally localize the parahippocampal place area (PPA) in the sighted group.

Experiment 1 — Size judgment

The participants were asked to perform size judgments on the objects that were referred to by the auditory words. There were three object categories — tools (e.g., 斧子 axe), large nonmanipulable objects (e.g., 帆船 sailboat) and animals (e.g., 青蛙 frog), each comprised of 30 items (see complete list in Supplementary Appendix). Tools included kitchen utensils, farm implements, weapons and other common indoor tools. Animals included mammals, birds, insects and reptiles. Following Mahon et al. (2009), large nonmanipulable objects included furniture (8, e.g., couch), appliances (6, e.g., refrigerator), vehicles (3, e.g., truck), buildings (3, e.g., castle) and other common objects (10, e.g., blackboard). All stimuli were disyllabic words and were matched across conditions on word frequency (log; tools: mean = .75, SD = 0.4; large nonmanipulable objects: mean = .77, SD = 0.6; animals: mean = .73, SD = 0.4; $F(2, 87) < 1$), familiarity (tools: mean = 5.5, SD = 1.1; large nonmanipulable objects: mean = 5.4, SD = 1.0; animals: mean = 5.1, SD = 0.7; $F(2, 87) = 1.1$, $p = .30$) and imageability (tools: mean = 6.7, SD = 0.4; large nonmanipulable objects: mean = 6.7, SD = 0.3; animals: mean = 6.7, SD = 0.2; $F(2, 87) < 1$). The familiarity and imageability ratings were collected from a group of 32 (16 for each rating) college students, who did not participate in the fMRI experiments, using a seven-point scale (seven for most familiar and most imageable). Each word was recorded digitally (22,050 Hz, 16 Bit) by a female native Mandarin speaker.

In the scanner, stimuli were presented binaurally over a headphone in blocks of five words, all from the same category. The participants were instructed to think about the size of the first item of the group, and to compare the subsequent items to the first one. If all of the five objects had roughly the same size, the participants responded by pressing a button with the index finger of the left hand; if at least one of the last four objects was different in size from the first one, the participants pressed a button with the right index finger. A response cue (auditory tone, duration 200 ms) was presented after the offset of the last item of the block, and the participants were asked to respond after hearing this response cue. Each of the five trials in a block lasted 2 s and the last trial was followed by a 4 s silent period for response. Thus, each block lasted 14 s, and was separated by a 14 s period of silence between blocks.

Each item was presented twice during the experiment and was grouped with different words for the two presentations. There were four runs: each lasted 4 min and 40 s and had 10 blocks. The first block of each run was used for practice. The order of blocks was constant for each participant and was pseudo-randomized with the restriction that no two consecutive blocks were from the same category.

Experiment 2 — Picture viewing

A passive picture-viewing task was conducted with the sighted individuals, using the items from the three main categories (tools, large nonmanipulable objects, and animals) in Experiment 1. Black and white photographs ($400 * 400$ pixels, visual angle $10.55° \times 10.55°$) were used in this experiment.

In the experiment the participants viewed the object photographs through a mirror attached to the head coil adjusted to allow foveal viewing of a back-projected monitor (refresh rate: 60 Hz; spatial resolution: 1024 × 768). The pictures were presented sequentially (666 ms; ISI = 0) in blocks of 30 items, all from the same category. Each block lasted approximately 20 s, followed by 20 s of fixation. The blocks were repeated four times in the experiment. The order of items within a block was constant across the participants, as was the order of the blocks. Consecutive blocks were never from the same category. This single-run task lasted 8 min and 10 s.

Experiment 3 — Scene localizer

We carried out a separate scene localizer experiment on the sighted participants who participated in the previous two experiments, and we were able to recruit back four participants. We selected black-and-white pictures of 30 scenes (300 * 300 pixels) and 30 objects (10 cars, 10 flowers and 10 chairs, 400 * 400 pixels). The stimuli were presented in 16 s blocks, separated by 10 s of fixation. Each block had 16 pictures, all from the same condition (each picture was presented for 800 ms, ISI = 200 ms). Scene and object blocks were presented in alternating fashion, with eight blocks of each condition occurring in one run of 7 min and 16 s long. The participants pressed a button with the left index finger rapidly whenever they saw two consecutive identical pictures. Each block and each category had an equal chance of having 0, 1, or 2 identical picture pairs.

MRI data acquisition

Structural and functional MRI data were collected with a 3 T Siemens Trio Tim scanner at the BNU MRI center. A high-resolution 3D structural data set was acquired with a 3D-MPRAGE sequence in the sagittal plane (TR: 2530 ms, TE: 3.39 ms, flip angle: 7°, matrix size: 256 × 256, 144 slices, voxel size: 1.33 × 1 × 1.33 mm, acquisition time: 8.07 min). BOLD signals were measured with an EPI sequence (TR: 2000 ms, TE: 30 ms, flip angle: 90°, matrix size: 64 × 64, voxel size: 3.125 × 3.125 × 4 mm, inter-slice distance: 4.6 mm, number of slices: 33; slice orientation: axial).

The scanning procedure for the blind group used the following order: a functional resting-state run for 6 min and 40 s; a 3D structural scan; the size judgment experiment. The sighted group underwent the same scan procedure as that for the blind participants except that ten participants did not receive the resting-state run. Furthermore, all sighted participants subsequently performed the passive picture viewing experiment at the end of the session. In the resting-state run, the participants were asked to lie still and not to think of anything in particular. In both the resting-state run and the auditory task runs the sighted participants were asked to keep their eyes closed. The scene localizer was carried out in another session more than three weeks later, which included one scene localizer run and a 3D structural scan. E-prime 1.1 (Schneider et al., 2002) was used for controlling stimulus presentation and recording responses.

fMRI data analysis

fMRI data were analyzed using BrainVoyager QX v2.3. The first 28 s in each run of the auditory size judgment task (the practice block) and 10 s in that of the passive picture-viewing task (fixation) were discarded. Preprocessing of the functional data included 3D motion correction with respect to the first (remaining) volume of the run scanned closest to the 3D structural data for each experiment, spatial smoothing (Gaussian filter, 6-mm Full Width Half Maximum), and temporal filtering (high-pass (GLM-Fourier): 3 sines/cosines for the one-back picture viewing experiment and 1 sines/cosines for other experiments). For each participant, functional data were then registered to her/his anatomical data. Finally, functional and anatomical volumes were transformed into a standardized space (Talairach and Tournoux, 1988), and functional data were resampled to 3 × 3 × 3 mm resolution.

All functional data were then analyzed using the general linear model (GLM). We included three predictors of interest corresponding to the three categorical conditions and six motion parameters as predictors of no interest.

We first carried out a whole-brain conjunction analysis for regions showing selectivity for large nonmanipulable objects: random-effect GLM analyses for large nonmanipulable objects > animals and large nonmanipulable objects > tools, each at the threshold of $p < .01$ uncorrected, cluster size > 7 resampled voxels, 189 mm^3, resulting in a conjunction threshold of $p < .001$ uncorrected. The cluster-level estimation for each contrast is adopted from the cluster-level statistical threshold estimator of BrainVoyager, based on the map's spatial smoothness and on an iterative procedure (Monte Carlo simulation with 1000 iterations). To quantify the relationship between the regions showing large nonmanipulable object selectivity and scene preference, we further carried out region-of-interest (ROI) analyses, defining ROIs using the full activation on the group level at $p < .05$ Bonferroni corrected, fixed effect and then carried out analyses using mean beta-values of different conditions for independent data sets in each ROI.

The functional connectivity of the resting-state data was analyzed using Statistical Parametric Mapping (SPM8, http://www.fil.ion.ucl.ac.uk/spm), the Resting-State fMRI Data Analysis Toolkit (REST, Song et al., 2011, http://www.restfmri.net) and Data Processing Assistant for Resting-State fMRI (DPARSF) (Yan and Zang, 2010). The first 10 volumes of the resting-state run of each participant were discarded for signal equilibrium and adaptation of the participants to the scanning noise. Next, slice timing and head motion correction were performed. A mean functional image was obtained for each participant, which was subsequently normalized to the EPI template. After the linear trend of the time courses was removed, a band-pass filter (0.01–0.08 Hz) was applied to reduce low-frequency drift and high-frequency noise. Finally, spatial smoothing (4-mm FWHM Gaussian kernel) was conducted to decrease spatial noise.

The functional connectivity was calculated by correlating the time series of each voxel with the seed region defined by the whole-brain contrasts. The seed region was obtained by creating a sphere with 6 mm radius around the peak seed voxel. Then, Fisher z-score transformations were conducted for the correlation coefficients to generate a z-FC map for each participant. To identify the regions showing significant functional connectivity with the seed(s), we did one sample *t*-tests on these individual z-FC maps to see whether they were significantly different from zero ($p < .05$, AlphaSim corrected). Only the regions showing positive correlations were presented.

The functional connectivity analyses were conducted on the gray matter mask generated using the following procedure. We included the voxels with a probability higher than 0.4 in the SPM5 template onto the gray matter mask. Given the signal distortion in cerebellum, we also excluded the cerebellar regions (#91–#116) in the Automated Anatomical Labeling (AAL) template (Tzourio-Mazoyer et al., 2002). In total, there were 36,272 voxels in the gray matter mask.

Results

Behavioral results

For the auditory size judgment experiment, the blind and the sighted participants respectively judged 30% (tools: 27%; animals: 35%; large nonmanipulable objects: 29%) and 32% (tools: 34%; animals: 30%; large nonmanipulable objects: 33%) of the blocks to be composed of items of roughly the same size. There was no difference between the participant groups ($t(28) < 1$). Because the participants were asked not to press the button until they heard the response cue, RTs were not particularly meaningful and were not analyzed further.

fMRI results

We have organized the fMRI results as follows: First we present whole-brain results for selectivity to large nonmanipulable objects using conjunction analyses of large nonmanipulable object > tool and large nonmanipulable > animal; We then compare the observed regions with regions defined in the sighted scene localizer task; Finally we show the resting-state functional connectivity patterns of the PPA region with the large nonmanipulable object selectivity. The overall task effects (all conditions versus baseline) in both participant groups (blind and sighted) are presented in the Supplementary material (Supplementary Results and Supplementary Fig. 1).

Whole-brain analyses testing for selectivity to large nonmanipulable objects

We first computed whole-brain (random effects) conjunction analyses of large nonmanipulable object > tool and large nonmanipulable > animal using the same threshold ($p < .01$ uncorrected, cluster size > 7 resampled voxels, 189 mm^3) in all experiments (Fig. 1a). In the sighted participants' picture viewing experiment, a bilateral medial VTC region close to PPA showed highly significant selectivity for large nonmanipulable objects. Bilateral transverse occipital sulcus (TOS) also showed large nonmanipulable object selectivity. Similar trends in bilateral retrosplenial complex (RSC) were observed without the cluster size threshold (i.e., $p < .01$ uncorrected). In the sighted participants' auditory experiment, bilateral PPA, bilateral RSC and left TOS showed selectivity for large nonmanipulable objects. In the blind participants' auditory experiment, similarly, bilateral PPA, bilateral RSC and left TOS showed significant selectivity for large nonmanipulable objects. Detailed information about the activation peak coordinates and cluster sizes is given in Table 1.

Relation between areas showing large nonmanipulable object selectivity and the parahippocampal place area

We further compared the results of the large nonmanipulable object selectivity to the results of a standard scene-selective cortex localizer. In the scene localizer task the participants performed a one-back picture viewing task on a set of widely used scene pictures. We functionally localized the scene areas by contrasting scene stimuli with varied objects (cars, chairs and flowers). The overall pattern in the visual cortex (Fig. 1b & Table 1; fixed effect analysis, $p < .05$ Bonferroni corrected) was similar to those of the large nonmanipulable object selectivity in both sighted and blind participants (Fig. 1a), including the strong activation of PPA. The peak Talairach coordinates were highly consistent across participants; S1: LH −28 −35 −12; RH 32 −44 −9; S2: LH −31 −38 −12; RH 23 −29 −18; S3: LH −25 −38 −12; RH 23 −41 −12; S4: LH −28 −44 −6; RH 23 −32 −9; all $p < .05$ Bonferroni corrected except for S4 RH $p < .05$ FDR corrected. These coordinates are also consistent with those reported previously in larger groups (e.g., Downing et al., 2006, LH −22 −47 −4; RH 23 −45 −5).

In order to quantify the similarity between the PPA regions showing specificity for scenes and for large nonmanipulable objects, we determined the degree of their overlap by calculating an overlap index, dividing the number of voxels common to two ROIs by the number of voxels of the smaller ROI. This denominator was chosen because the index would thus be less influenced by relative size differences between ROIs compared to other possibilities (e.g., the average size or the unique voxels in the two ROIs) (Bracci et al., 2012). The thresholds were set to $p < 0.05$ (Bonferroni corrected; fixed effect) for the scene localizer to separate PPA ROIs from those extending to elsewhere, and $p < .01$ (uncorrected, cluster size > 7 resampled voxels, 189 mm^3; random effect; resulting in a conjunction threshold of $p < .001$) for each contrast of the conjunction results of large nonmanipulable objects selectivity (large nonmanipulable > tool and large nonmanipulable > animal) in the sighted group's auditory, the blind group's auditory, and the sighted group's picture-viewing experiments. The left and right hemisphere ROIs were collapsed. Considerable overlap was found between scene and large nonmanipulable category responses in the sighted group's auditory (45% overlap), the blind group's auditory (58% overlap) and the sighted group's picture-viewing experiments (65% overlap). We also computed the overlap index adopting similar thresholds for both ROIs, that is, using a $p < .001$ uncorrected, cluster size > 7 resampled voxels (189 mm^3) threshold for the scene localizer experiment (ROI size 14,789 mm^3). The overlap indexes were 63% (with sighted group's auditory experiment), 72% (with blind group's auditory experiment) and 77% (with sighted group's picture viewing experiment) respectively.

We further performed ROI analyses in the PPA regions obtained in the scene localizer experiment ($p < 0.05$ Bonferroni corrected; fixed effect; Fig. 1b) to examine if they showed specificity for large nonmanipulable objects. For the auditory experiment, we conducted an ANOVA with hemisphere (left, right) and category (tool, animal, large nonmanipulable object) as within subject factors and participant group (blind, sighted) as a between subject factor. The main effect of the category was significant ($F(2, 27) = 43.7$, $p < .0001$), with large nonmanipulable object responses higher than both tools (post hoc comparisons: $p < .0001$) and animals (post hoc comparisons: $p < .0001$), and no difference between responses to tools and animals (post hoc comparisons: $p = .61$). Thus, the PPA region that was sensitive to scene stimuli also preferred large nonmanipulable objects over tools and animals. The main effect of the hemisphere was significant ($F(1, 28) = 7.7$, $p < .05$), with overall stronger activation in the left hemisphere than in the right hemisphere. The main effect of the group was marginally significant ($F(1, 28) = 4.1$, $p = .05$), with overall stronger responses in blind than in sighted participants. The interaction between category and hemisphere/group was not significant ($F_{category * hemisphere}(2, 27) = 2.1$, $p = .15$; $F_{category * group}(2, 27) = 1.5$, $p = .23$), suggesting that the categorical pattern was similar for blind and sighted participants.

Given the lack of significant interactions between the category and the hemisphere, we present the category responses collapsing across hemispheres for the sighted group's auditory and the blind group's auditory experiments in the PPA ROIs (Figs. 2a–b).

For the picture-viewing experiment, we conducted an ANOVA with hemisphere (left, right) and category (tool, animal, large nonmanipulable object) as two within subject factors. The main effect of category was significant ($F(2, 14) = 22.1$, $p < .0001$), with higher responses to large nonmanipulable objects than to both tools (post hoc comparisons: $p < .0001$) and animals (post hoc comparisons: $p < .0001$), and no difference between responses to tools and animals (post hoc comparisons: $p = .27$). The main effect of hemisphere was significant ($F(1, 15) = 25.5$, $p < .0001$), with overall stronger activation in the left than in the right hemisphere. The interaction between category and hemisphere was also significant ($F(2, 14) = 5.8$, $p < .05$). Examining the comparisons among categories in each hemisphere separately, we found that in both hemisphere ROIs, large nonmanipulable objects evoked higher BOLD response than both tools (left ROI: $t(15) = 5.8$, $p < .0001$; right ROI: $t(15) = 7.0$, $p < .0001$) and animals (left ROI: $t(15) = 6.3$, $p < .0001$; right ROI: $t(15) = 4.5$, $p < .001$). The difference between responses to tools and animals was not significant in left ROI ($t(15) < 1$),

Fig. 1. Results of whole-brain random-effect conjunction analyses showing selectively for nonmanipulable objects in VTC and the whole-brain fixed-effects analysis for the scene localizer. a) Shown here is the conjunction of the contrasts nonmanipulable objects > animals and nonmanipulable objects > tools separately for the three experiments: the sighted group's auditory experiment (the upper panel), the blind group's auditory experiment (the middle panel) and the sighted group's picture viewing experiment (the lower panel) (all ps < .01 uncorrected, cluster size > 7 resampled voxels, 189 mm^3). Voxels showing stronger BOLD responses for nonmanipulable stimuli are shown on the red–yellow color scale. The results were superimposed on one participant's brain. b) Shown here is the contrast of scenes > objects (cars, chairs and flowers) for four of the sighted participants performing the scene localizer task ($p < .05$ Bonferroni corrected; fixed effect). Voxels showing stronger BOLD responses for the scene stimuli are shown on the red–yellow color scale. The results were superimposed on one participant's brain.

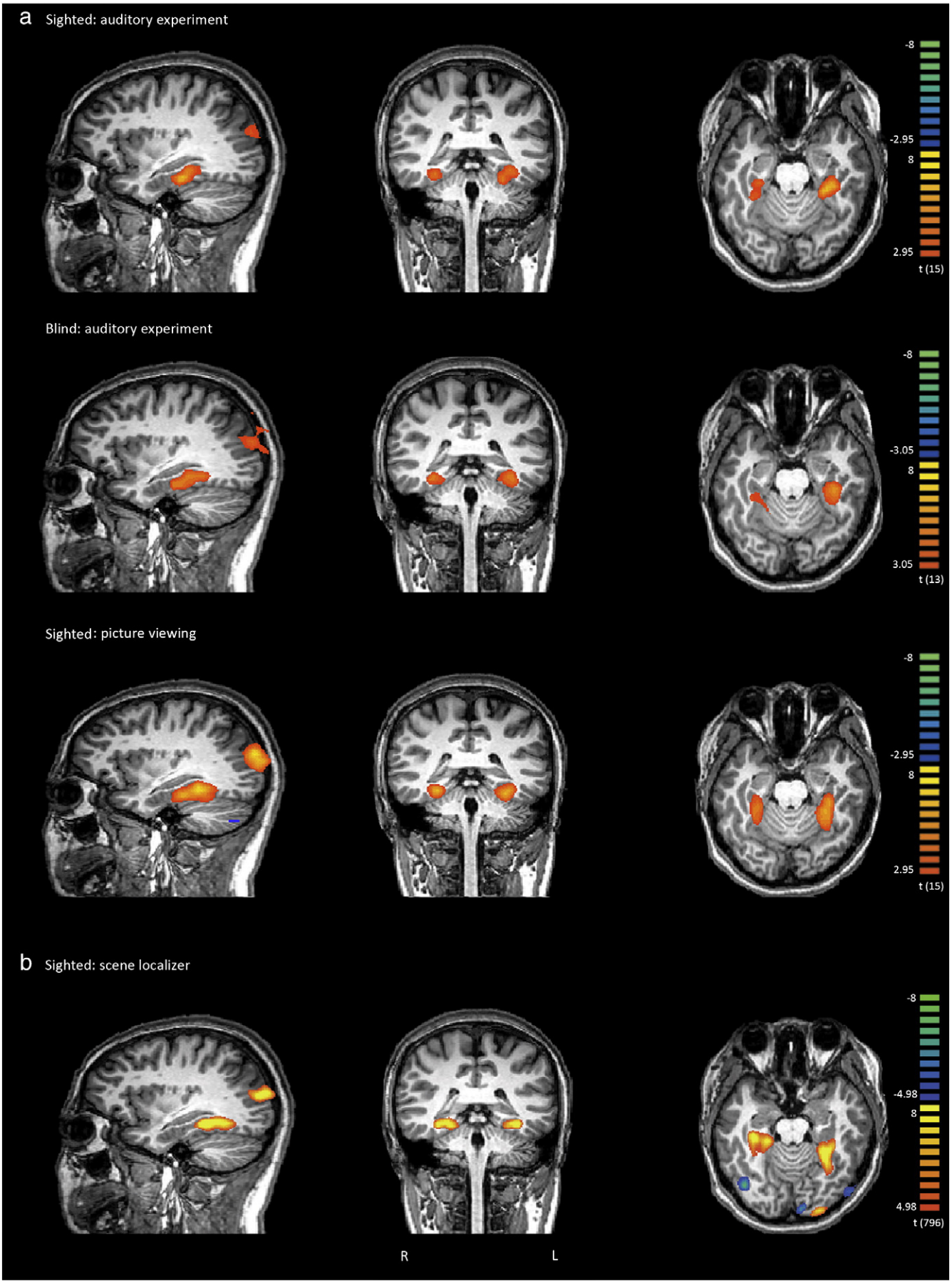
a
Sighted: auditory experiment
-8
-2.95
8
2.95
t (15)
Blind: auditory experiment
-8
-3.05
8
3.05
t (13)
Sighted: picture viewing
-8
-2.95
8
2.95
t (15)
b
Sighted: scene localizer
-8
-4.98
8
4.98
t (796)
R
L

Table 1
Peak TAL coordinates (cluster size) of brain regions obtained in whole-brain results for conjunction analyses of large nonmanipulable object > tool and large nonmanipulable object > animal ($p < .01$ uncorrected, cluster size > 7 resampled voxels, 189 mm^3 for each contrast), and for scene > object in the scene localizer experiment ($p < .05$ Bonferroni corrected; fixed effect).

	Large nonmanipulable object selectivity			Scene localizer
	Sighted size judgment	Blind size judgment	Sighted viewing	Sighted viewing
Left PPA	−28 −26 −21 (3437 mm^3)	−34 −29 −15 (4175 mm^3)	−28 −41 −15 (5338 mm^3)	−28 −38 −12 (3913 mm^3)
Right PPA	29 −35 −15 (1376 mm^3)	29 −32 −12 (1472 mm^3)	29 −38 −15 (3296 mm^3)	32 −38 −9 (3924 mm^3)
Left RSC	−16 −59 12 (1554 mm^3)	−22 −59 9 (1204 mm^3)	–	−19 −59 9 (402 mm^3)
Right RSC	20 −59 15 (511 mm^3)	17 −50 3 (580 mm^3)	–	17 −53 15 (1732 mm^3)
Left TOS	−28 −80 21 (1227 mm^3)	−43 −80 18 (3816 mm^3)	−34 −86 9 (4335 mm^3)	−31 −83 15 (3575 mm^3)
Right TOS	–	–	32 −89 18 (4277 mm^3)	35 −80 21 (6221 mm^3)
Left inferior occipital gyrus	–	–	–	−22 −92 −15 (724 mm^3)
Left precuneus	–	–	–	−13 −77 39 (649 mm^3)
Right precuneus	–	–	–	14 −74 36 (1481 mm^3)
Left middle frontal gyrus	–	–	–	−25 −2 51 (217 mm^3)
Right middle frontal gyrus	–	–	–	32 −8 57 (988 mm^3)
Right middle frontal gyrus	–	–	–	47 19 36 (638 mm^3)

but it was marginally significant in right ROI ($t(15) = 1.9$, $p = .07$) with higher response to animals than to tools (Figs. 2c–d).

Intrinsic functional connectivity patterns of the regions showing large nonmanipulable object selectivity

We explored the intrinsic functional connectivity patterns of regions showing category specificity for large nonmanipulable objects. We used the observed peak coordinates in PPA obtained in the above conjunction analyses (large nonmanipulable object > tool and large nonmanipulable object > animal, for sighted auditory experiment and blind auditory experiment), and calculated the correlation between the time series of the seed regions and all other voxels in the brain from the resting-state data. For the sighted participants (seven individuals), the left PPA ROI was found to be significantly connected with the right PPA, bilateral RSC, left anterior temporal lobe, and bilateral medial frontal gyrus. The right PPA ROI was significantly connected with the left PPA, right TOS, bilateral RSC, right anterior temporal lobe, and right medial frontal gyrus (Fig. 3; $p < .05$ AlphaSim corrected). For the blind group, we observed that the left PPA ROI showed significant functional connectivity with the right PPA, right TOS, bilateral RSC, right anterior temporal lobe, bilateral medial frontal gyrus, and right superior temporal gyrus. The right PPA ROI showed significant functional connectivity with the left PPA, bilateral TOS, bilateral RSC, right fusiform gyrus, right middle frontal gyrus, and bilateral anterior temporal lobe (Fig. 3; $p < .05$ AlphaSim corrected).

Discussion

In the present study, we explored the pattern of object selectivity in PPA in congenitally blind participants and sighted participants using an auditory object size judgment task and a picture-viewing task performed by the sighted participants. We found that in sighted participants performing the picture-viewing task and both sighted and blind participants performing the auditory task, there was selectivity for large nonmanipulable objects relative to both tools and animals in PPA, although sighted participants performing the auditory task showed overall weaker activity than blind participants. Similar results were obtained in RSC and TOS. Furthermore, the PPA region showing selectivity for large nonmanipulable objects was functionally connected with RSC and TOS during the resting-state scan in both sighted and blind groups.

It is well documented that compared to common objects or faces, stimuli related to scenes, places, buildings or landmarks evoke stronger activation in the areas PPA, TOS, and RSC (e.g., Epstein, 2008; Epstein and Kanwisher, 1998; Epstein et al., 2007), the regions in which we observed selectivity to large nonmanipulable objects. Our results are consistent with a series of recent studies that reported stronger activity in these regions for objects that are large or nonportable (e.g., Konkle and Oliva, 2012; Mullally and Maguire, 2011). Our observation of the overall effect of stronger activation in the blind group relative to the sighted group in the auditory size judgment task is also in line with the literature that sighted participants doing non-visual tasks show minimal or even negative activation in the visual cortex (e.g., Laurienti et al., 2002), while congenitally blind adults recruit visual areas for non-visual tasks (e.g., Amedi et al., 2004). Importantly, our results show for the first time that selectivity to large nonmanipulable objects in PPA and other scene-related regions (RSC and TOS) is independent of visual experience and input modality. These findings challenge theories that assume that the effects observed in these regions are driven by visual properties of scenes or objects. For instance, it has been proposed that the selectivity for scenes and large objects may be driven by the type of visual experience typically associated with these categories (e.g., Hasson et al., 2002; Levy et al., 2001; see also Konkle and Oliva, 2012). Specifically, the perception of scenes (and by extension, large objects) requires large-scale integration of peripheral visual input. As such, it has been hypothesized that PPA selectivity may develop from feed-forward projections of earlier visual regions that are sensitive to the peripheral visual field. Our results in congenitally blind participants show that purely feed-forward, visually-driven accounts cannot fully explain the development of large object selectivity in PPA.

Other types of variables being proposed to modulate PPA/RSC/TOS responses need not be exclusively visual, and could be extended to explain the similarity between blind and sighted participants, including the extent to which a sense of space can be evoked by the stimuli, the real-world size of the stimuli, or the richness of contextual associations (e.g., Bar, 2004; Bar and Aminoff, 2003; Konkle and Oliva, 2012; Mullally and Maguire, 2011). These variables are often inter-correlated and have been argued to affect the scene-processing regions by evoking spatial navigation processing — the more useful an object is for navigation, the stronger the PPA/RSC/TOS activation (e.g., Epstein, 2008; Epstein and Ward, 2010; Epstein et al., 1999; Troiano et al, in press). Large nonmanipulable objects tend to be more useful as landmarks (e.g., refrigerator in a house), whereas smaller objects or animals tend to be mobile and thus less useful as landmarks. It is conceivable that the navigation-relevant properties of objects can be obtained and used through navigation experience with multiple modalities. Blind individuals may associate large nonmanipulable objects with spatial navigation through auditory and tactile experiences. Whether navigation-relevance is the organizational principal of the scene-related regions still warrants further investigation. Our current results with congenitally blind (and auditory words with sighted participants) nonetheless suggest that the information being processed in the scene-selective regions (PPA, RSC, and TOS) is not fully visually driven.

A previous study (Mahon et al., 2009) reported a preference for inanimate objects (combined response to large nonmanipulable objects and tools) over animate objects in both sighted and three congenitally blind participants in the medial portion of bilateral VTC, an area highly similar to the PPA region showing selectivity for large nonmanipulable

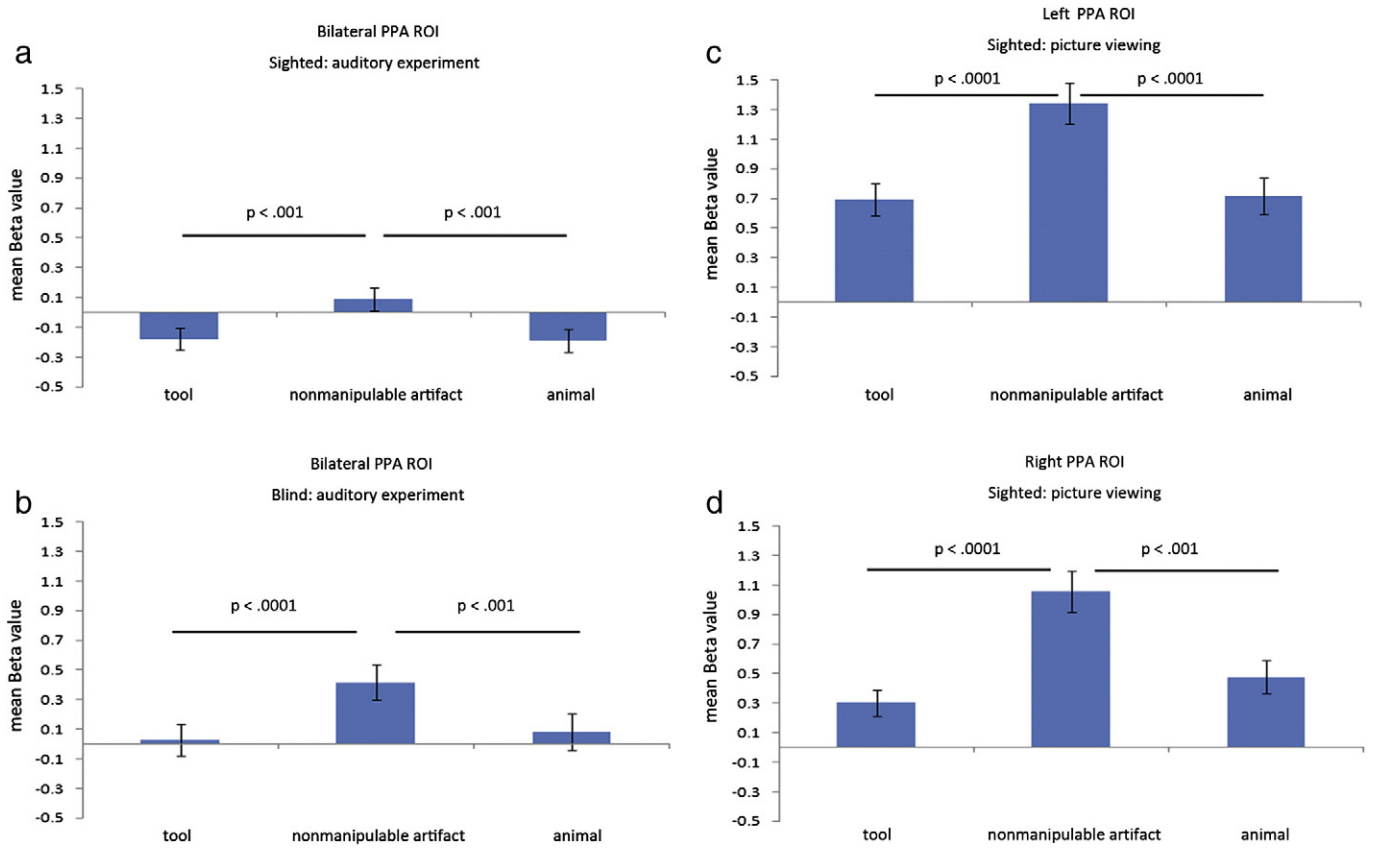

Fig. 2. Responses to the three object categories in bilateral PPA defined by the scene localizer. PPA was defined by contrasting scenes against other common objects in four sighted participants ($p < .05$ Bonferroni corrected; fixed effect); a–d) For the sighted group's auditory experiment, the blind group's auditory experiment and the sighted group viewing pictures, beta values for each category were plotted. The bar graphs depict the average beta values of each category within the bilateral PPA ROI. Error bars reflect the standard error of the mean.

objects in the current study. In additional analyses, we replicated this finding (see Supplementary material). When taking this "inanimate" region as ROI, we found that in both blind (auditory experiment) and sighted groups (picture viewing experiment), large nonmanipulable objects evoked significantly higher BOLD responses compared to the other two categories, while there was no difference between the activation to tools and animals (Supplementary material). These additional results thus suggest a re-interpretation of the inanimate preference reported previously (Mahon et al., 2009), showing that selectivity was specifically driven by the large nonmanipulable objects rather than by inanimate objects more generally.

A further interesting data point regarding the animacy effect was observed in this analysis: Animals evoked significantly higher activation in the bilateral occipital temporal cortex and the right fusiform gyrus compared to tools and large nonmanipulable objects in the sighted group's picture viewing experiment. However, when using these brain regions as ROIs, we did not find any difference between response to animals and to other two categories in both groups' auditory experiments (Supplementary material and Supplementary Fig. 3). This finding differed somewhat from Mahon et al. (2009), who reported a small cluster in left lateral occipital cortex in which similar animate > inanimate effects were observed in the sighted group performing visual and auditory tasks, and the blind participants performing auditory experiments. Note, however, that those results were observed using fixed effect analyses at a lenient statistical threshold ($p < .05$, uncorrected for multiple comparisons). It is possible that their observations may not generalize to other participants. Our finding of weak (or even absent) animal selectivity in the auditory experiment in both sighted and blind participants contrasts with the input-independent large nonmanipulable artifact selectivity, and suggests an interesting interaction between object domains and input modalities, at least in the sighted participants. Selectivity for animals has previously been shown to be modality-specific. The effects were rarely present when the stimuli were written or auditory words instead of pictures (Devlin et al., 2005; Price et al., 2003; but see Chao et al., 1999). Adam and Noppeney (2010), using visual stimuli, localized VTC regions showing animal (fusiform gyrus) or place (PPA) selectivity and then measured responses to animal and place sounds, such as "meow" for cat. They found that the PPA was selective for landmark sounds, but that the fusiform gyrus did not respond selectively to animal sounds. Thus, it is possible that animal selectivity in VTC is primarily driven by the specific visual characteristics of animals; words, or even stimuli directly denoting non-visual sensory features associated with animals, may not be strong enough to activate visual representations.

Our group comparison results highlighted the striking similarity between sighted and blind participants. In particular, the selectivity for large nonmanipulable objects near the parahippocampal place area was comparable not only between sighted and blind participants in the auditory task, they were also similar to sighted participants performing picture viewing experiment. These results are in line with a series of recent studies showing the similarity of activation profiles between blind and sighted individuals. For example, Reich et al. (2011) reported that blind individuals showed selective responses to Braille word stimuli in a region corresponding to the visual word form area in sighted individuals; Collignon et al. (2011) found that the activation profiles in spatial processing regions of dorsal occipital cortex were similar between blind individuals processing auditory spatial stimuli and sighted individuals processing visual spatial stimuli (see also Kupers et al., 2010 for similar results for blind participants performing a navigation task). While it is possible that the

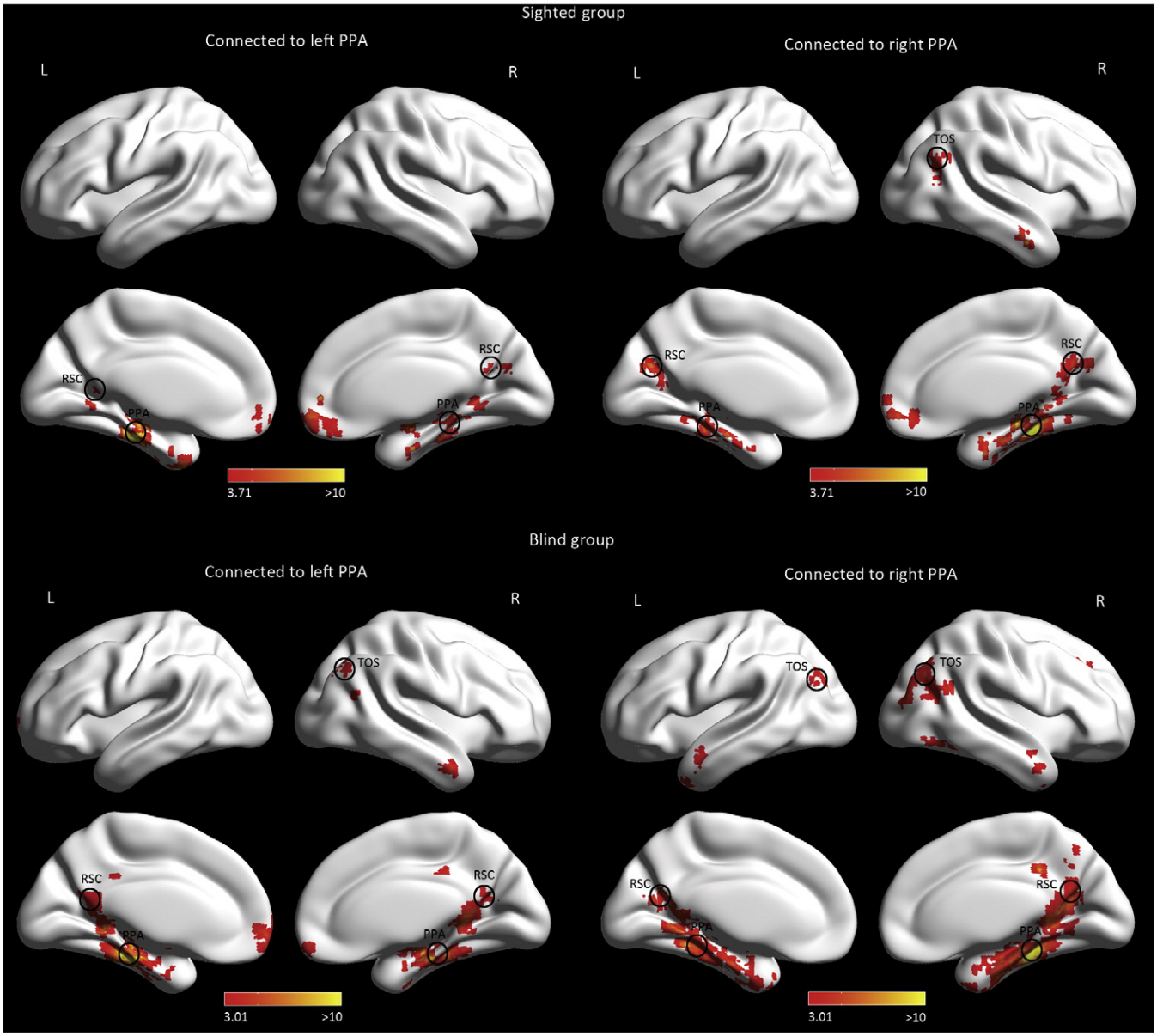

Fig. 3. Functional connectivity of the resting-state data. For the sighted group, the seed regions (bilateral PPA) were defined by the conjunction of large nonmanipulable object > tool & large nonmanipulable object > animal in sighted group's auditory experiment. For the blind participants, the seed regions (bilateral PPA) were defined by the conjunction of large nonmanipulable object > tool & large nonmanipulable object > animal in blind group's auditory experiment. The whole-brain functional connectivity with the seed regions was calculated voxel by voxel ($p < .05$ AlphaSim corrected). Voxels showing significant positive functional connectivity with the seed regions are shown on the red–yellow color scale.

specific content of the representations in the visual cortex of congenitally blind individuals is different from that in sighted individuals (e.g., visual imagery), it is more parsimonious to assume that at least part of the organization of higher-level visual cortex is independent of visual experience (Mahon and Caramazza, 2011).

Finally, the similar resting-state functional connectivity patterns associated with PPA in the sighted and the blind groups provide new insights into the potential mechanisms for PPA's functional profile. While accumulating evidence has shown that scene or navigation related tasks co-activate PPA, RSC and TOS (e.g., Epstein, 2008), which is commonly referred to as the "scene network", our study shows for the first time that PPA is intrinsically connected with RSC and TOS even in the absence of any explicit task requirements. The finding that this intrinsic network is independent of visual experience, in association with the similar functional selectivity for large nonmanipulable objects in these regions, is in line with the theoretical proposal that the categorical organization within VTC is partly driven by differential connectivity with other functionally relevant brain regions (Mahon and Caramazza, 2011; Mahon et al., 2007). The exact role of these intrinsic connections in object processing and whether these connections are modulated by specific tasks differently in sighted and blind participants warrant further investigation.

To conclude, we observed selectivity for large nonmanipulable objects relative to animals and tools in PPA in both sighted (picture viewing and auditory) and congenitally blind participants (auditory), with similar patterns also observed in two additional scene-selective regions in TOS and RSC. These regions are intrinsically connected with each other, in both blind and sighted groups, and may be sensitive to information related to navigation that is independent of visual experience. More generally, the highly similar categorical organization in individuals with and without visual experience, when performing identical task, suggests that the large-scale organization of high-order visual cortex may not be primarily shaped by visual input.

Funding

This work was supported by the 973 Program (2013CB837300), the NSFC (31171073; 31222024; 31271115), and the Fondazione Cassa di Risparmio di Trento e Rovereto.

Supplementary data to this article can be found online at http://dx.doi.org/10.1016/j.neuroimage.2013.04.051.

Acknowledgments

We thank Xueming Lu for his assistance in data analyses, and all BNU-CNLab members for their aids in data collection.

Conflict of interest statement

No author has any conflict of interest with respect to this article.

References

Adam, R., Noppeney, U., 2010. Prior auditory information shapes visual category-selectivity in ventral occipito-temporal cortex. NeuroImage 52, 1592–1602.
Amedi, A., Floel, A., Knecht, S., Zohary, E., Cohen, L.G., 2004. Transcranial magnetic stimulation of the occipital pole interferes with verbal processing in blind subjects. Nat. Neurosci. 7, 1266–1270.
Bar, M., 2004. Visual objects in context. Nat. Rev. Neurosci. 5, 617–629.
Bar, M., Aminoff, E., 2003. Cortical analysis of visual context. Neuron 38, 347–358.
Bracci, S., Ietswaart, M., Peelen, M.V., Cavina-Pratesi, C., 2010. Dissociable neural responses to hands and non-hand body parts in human left extrastriate visual cortex. J. Neurophysiol. 103, 3389–3397.
Bracci, S., Cavina-Pratesi, C., Ietswaart, M., Caramazza, A., Peelen, M.V., 2012. Closely overlapping responses to tools and hands in left lateral occipitotemporal cortex. J. Neurophysiol. 107, 1443–1456.
Chao, L.L., Haxby, J.V., Martin, A., 1999. Attribute-based neural substrates in temporal cortex for perceiving and knowing about objects. Nat. Neurosci. 2, 913–919.
Cohen, L., Dehaene, S., 2004. Specialization within the ventral stream: the case for the visual word form area. NeuroImage 22, 466–476.
Collignon, O., Vandewalle, G., Voss, P., Albouy, G., Charbonneau, G., Lassonde, M., Lepore, F., 2011. Functional specialization for auditory–spatial processing in the occipital cortex of congenitally blind humans. Proc. Natl. Acad. Sci. U. S. A. 108, 4435–4440.
Devlin, J.T., Rushworth, M.F.S., Matthews, P.M., 2005. Category-related activation for written words in the posterior fusiform is task specific. Neuropsychologia 43, 69–74.
Downing, P.E., Jiang, Y., Shuman, M., Kanwisher, N., 2001. A cortical area selective for visual processing of the human body. Science 293, 2470–2473.
Downing, P.E., Chan, A.W., Peelen, M.V., Dodds, C.M., Kanwisher, N., 2006. Domain specificity in visual cortex. Cereb. Cortex 16, 1453–1461.
Epstein, R.A., 2008. Parahippocampal and retrosplenial contributions to human spatial navigation. Trends Cogn. Sci. 12, 388–396.
Epstein, R.A., Kanwisher, N., 1998. A cortical representation of the local visual environment. Nature 392, 598–601.
Epstein, R.A., Ward, E.J., 2010. How reliable are visual context effects in the parahippocampal place area? Cereb. Cortex 20, 294–303.
Epstein, R.A., Harris, A., Stanley, D., Kanwisher, N., 1999. The parahippocampal place area: recognition, navigation, or encoding? Neuron 23, 115–125.
Epstein, R.A., Higgins, J.S., Jablonski, K., Feiler, A.M., 2007. Visual scene processing in familiar and unfamiliar environments. J. Neurophysiol. 97, 3670–3683.
Goh, J.O.S., Siong, S.C., Park, D., Gutchess, A., Hebrank, A., Chee, M.W.L., 2004. Cortical areas involved in object, background, and object-background processing revealed with functional magnetic resonance adaptation. J. Neurosci. 24 (45), 10223–10228.
Hasson, U., Levy, I., Behrmann, M., Hendler, T., Malach, R., 2002. Eccentricity bias as an organizing principle for human high-order object areas. Neuron 34, 479–490.
Kanwisher, N., 2010. Functional specificity in the human brain: a window into the functional architecture of the mind. Proc. Natl. Acad. Sci. U. S. A. 107, 11163–11170.
Kanwisher, N., McDermott, J., Chun, M.M., 1997. The fusiform face area: a module in human extrastriate cortex specialized for face perception. J. Neurosci. 17, 4302–4311.
Konkle, T., Oliva, A., 2012. A real-world size organization of object responses in occipito-temporal cortex. Neuron 74 (6), 1114–1124.
Kravitz, D.J., Peng, C.S., Baker, C.I., 2011. Real-world scene representations in high-level visual cortex: it's the spaces more than the places. J. Neurosci. 31 (20), 7322–7333.
Kupers, R., Chebat, D.R., Madsen, K.H., Paulson, O.B., Ptito, M., 2010. Neural correlates of virtual route recognition in congenital blindness. Proc. Natl. Acad. Sci. U. S. A. 107, 12716–12721.
Laurienti, P.J., Burdette, J.H., Wallace, M.T., Yen, Y.F., Field, A.S., Stein, B.E., 2002. Deactivation of sensory-specific cortex by cross-modal stimuli. J. Cogn. Neurosci. 14 (3), 420–429.
Levy, I., Hasson, U., Avidan, G., Hendler, T., Malach, R., 2001. Center-periphery organization of human object areas. Nat. Neurosci. 4, 533–539.
Maguire, E.A., Frith, C.D., Cipolotti, L., 2001. Distinct neural systems for the encoding and recognition of topography and faces. NeuroImage 13, 743–750.
Mahon, B.Z., Caramazza, A., 2011. What drives the organization of object knowledge in the brain? Trends Cogn. Sci. 15, 97–103.
Mahon, B.Z., Milleville, S.C., Negri, G.A., Rumiati, R.I., Caramazza, A., Martin, A., 2007. Action-related properties shape object representations in the ventral stream. Neuron 55, 507–520.
Mahon, B.Z., Anzellotti, S., Schwarzbach, J., Zampini, M., Caramazza, A., 2009. Category-specific organization in the human brain does not require visual experience. Neuron 63, 397–405.
Mullally, S.L., Maguire, E.A., 2011. A new role for the parahippocampal cortex in representing space. J. Neurosci. 31, 7441–7449.
Park, S., Brady, T.F., Greene, M.R., Oliva, A., 2011. Disentangling scene content from spatial boundary: complementary roles for the parahippocampal place area and lateral occipital complex in representing real-world scenes. J. Neurosci. 31 (4), 1333–1340.
Peelen, M.V., Downing, P.E., 2005. Selectivity for the human body in the fusiform gyrus. J. Neurophysiol. 93, 603–608.
Pietrini, P., Furey, M.L., Ricciardi, E., Gobbini, M.I., Wu, W.H.C., Cohen, L., Guazzelli, M., Haxby, J.V., 2004. Beyond sensory images: object-based representation in the human ventral pathway. Proc. Natl. Acad. Sci. U. S. A. 101, 5658–5663.
Price, C.J., Noppeney, U., Phillips, J., Devlin, J.T., 2003. How is the fusiform gyrus related to category-specificity? Cogn. Neuropsychol. 20, 561–574.
Reich, L., Szwed, M., Cohen, L., Amedi, A., 2011. A ventral visual stream reading center independent of visual experience. Curr. Biol. 21, 363–368.
Ross, M.G., Oliva, A., 2010. Estimating perception of scene layout properties from global image features. J. Vis. 10 (1), 2.1–2.25.
Save, E., Cressant, A., Thinus-Blanc, C., Poucet, B., 1998. Spatial firing of hippocampal place cells in blind rats. J. Neurosci. 18 (5), 1818–1826.
Schneider, W., Eschman, A., Zuccolotto, A., 2002. E-Prime Reference Guide. Psychology Software Tools, Inc., Pittsburgh.
Song, X., Dong, Z., Long, X., Li, S., Zuo, X., Zhu, C., He, Y., Yan, C., Zang, Y., 2011. REST: a toolkit for resting-state functional magnetic resonance imaging data processing. PLoS One 6 (9), e25031.
Talairach, J., Tournoux, P., 1988. Co-planar Stereotaxic Atlas of the Human Brain. Thieme Medical Publishers, New York.
Troiani, V., Stigliani, A., Smith, M.E., Epstein, R.A., 2013. Multiple object properties drive scene-selective regions. Cereb. Cortex. http://dx.doi.org/10.1093/cercor/bhs364 (Dec 4. Epub ahead of print, in press).
Tzourio-Mazoyer, N., Landeau, B., Papathanassiou, D., Crivello, F., Etard, O., Delcroix, N., Mazoyer, B., Joliot, M., 2002. Automated anatomical labeling of activations in SPM using a macroscopic anatomical parcellation of the MNI MRI single-subject brain. Neuroimage 15, 273–289.
Wolbers, T., Klatzky, R.L., Loomis, J.M., Wutte, M.G., Giudice, N.A., 2011. Modality-independent coding of spatial layout in the human brain. Curr. Biol. 21, 984–989.
Yan, C., Zang, Y., 2010. DPARSF: a MATLAB toolbox for "pipeline" data analysis of resting-state fMRI. Front. Syst. Neurosci. 4, 13.